INTERNATIONAL JOURNAL OF
COASTAL, OFFSHORE & ENVIRONMENTAL ENGINEERING IJCOE Vol.10/No. 2/ Spring 2025 (45-53)

Available online at: www. Ijcoe.org

Analyzing the Impact of Non-Dimensional Hydrodynamic Coefficients on the Performance of Oscillating Wave Surge Converters

Ghazale Sadripour[1], Rouzbeh Shafaghat[2*], Behrad Alizadeh Kharkeshi[3]

1 PhD student in Mechanical Engineering, Sea-Based Energy Research Group, Babol Noshirvani University of Technology, Babol, Iran, ghazale.sadripour@gmail.com

2 Professor in Mechanical Engineering, Sea-Based Energy Research Group, Babol Noshirvani University of Technology, Babol, Iran, rshafaghat@nit.ac.ir*

3 Assistant Professor in Mechanical Engineering, Sea-Based Energy Research Group, Babol Noshirvani University of Technology, Babol, Iran, b.alizadeh@nit.ac.ir

ARTICLE INFO

Article History:
Received:26 Oct 2024
Accepted: 06 Aug 2025
Available online ….

Keywords:
Renewable energy
Caspian Sea
OWSC
Experimental study
Frequency

ABSTRACT

Applying renewable energy could decrease the side effects of fossil fuels, therefore wave energy converters are crucial for implementing. This study focuses on the experimental investigation of an OWSC (1:8) by considering Caspian Sea for installation. After defining the significant hydrodynamic coefficients that impact the performance of the OWSC, including damping, pressure, and transmission coefficients, this study identified the parameters influencing these coefficients and investigated how these parameters affected them. The experiments were designed within the range of wave heights [0.04-0.1] m, wave frequency [0.4-0.63] Hz and water depths [0.8-1.5] m. Previous studies have shown that draft depth, wave height, and wave frequency are parameters affecting the performance of WEC. In this paper, the effect of these parameters on the hydrodynamic coefficients of the WEC was investigated. The results showed that increasing the wave height decreases the damping coefficient of the WEC, it was also shown that the effect of the dimensionless draft depth on the damping coefficient has a non-linear behavior and the WEC has the lowest damping coefficient at the optimal draft depth. An increase in the wave height leads to a decrease in the pressure coefficient (Cp), the Cp decreases by approximately 40% when the wave height changes from 0.04 to 0.1 m. The effect of the dimensionless wave frequency on the Cp is insignificant. Increasing the dimensionless draft depth leads to an increase in the transfer coefficient (Ct). Furthermore, the results of the correlation between parameters and Hydrodynamic coefficients indicate correlation of approximately -1 between wave height and Cp, close to -1 between wave height and Cd, and a close to 0 between wave height and Ct.

1. Introduction

In recent years, several energy sources have been introduced and are being exploited. The growth in population, the rise in energy demand, limitations of fossil fuel resources, and the problems associated with their consumption, such as increased CO2 emissions in the atmosphere, climate change, global warming, etc., have led scientists to utilize clean and renewable energy sources. Among these sources such as solar energy, wind energy, biomass energy, geothermal energy, and wave energy can be mentioned. Between the mentioned renewable energies, wave energy is particularly notable due to its advantages such as high energy density, significant storage capacity, lack of pollution, and preservation of underground resources [1]. With two-thirds of the Earth's surface covered by oceans, harnessing ocean energy could be an important source of green energy for coastal communities [2]. The essential requirement for absorption of wave energy is the presence of a device capable of absorbing the maximum amount of energy from the waves upon their impact. In the world of renewable energies, WECs are among the newest technologies [3]. WECs come in various types, and each of these WECs utilizes a different range of power generation mechanisms.

OWSC is a novel WEC designed to be installed in near shore and shallow water areas (depth of 10-20 m). In shallow waters, the motion of water particles is predominantly horizontal. OWSCs are specifically designed to effectively interact with the horizontal movement of particles, allowing for a large amplitude of motion working surface area and minimizing energy losses. The OWSC consists of a flap that rotates around a horizontal axis, either above the water surface or near the seabed, perpendicular to the direction of wave propagation [4]. Lots of research has been carried out on wave energy, and in most cases, energy extraction systems have been developed on a laboratory scale. These systems have been tested under simulated ocean conditions, and some of them have progressed to the operational phase. Drew et al. [5] in 2009, investigated the overall status of wave energy, specifically focusing on the various WEC technologies, with an emphasis on projects being carried out in the United Kingdom. Babarit et al. [6] in 2012, by analyzing the annual power output of several converters, were able to extract cost-related performance parameters. Renzi and Dias [7] in 2013 conducted an analytical study of an OWSC, utilizing a semi-analytical model of the potential flow. They derived correlations between the hydrodynamic parameters of the system through their study. Their parametric study showed that the excitation torque and added moment of inertia increase with a growing in flap width. Their results also demonstrated that an increase in flap width has a significant impact on the energy absorption coefficient. Sarkar et al. [8] in 2013 analytically investigated the OWSC efficiency by considering six different wave conditions. The modeling was performed using the potential flow theory and Green's theorem. They conducted a comparison between the performances of two WECs with different widths. The results indicate the importance of width on the power capture. A WEC with a smaller width has a higher power capture coefficient under the effect of waves with a shorter wavelength. This is because the excessive widening of a WEC limits its energy absorption under the effect of waves with a short wavelength. Furthermore, due to increased added moment of inertia, a flap with a larger width has a higher power capture coefficient under the effect of waves with longer wavelengths. Wei et al. [9] in 2013 proposed the use of finite volume and dynamic mesh methods to simulate wave forces on an OWSC exposed to waves. The outcomes revealed that the numerical model with dynamic mesh can be used for modeling the motion large amplitude of a flap. Renzi et al. [10] in 2014 performed numerical and semi-analytical modeling (inviscid potential flow theory) OWSC arrays in wave energy farm. They calculated the hydrodynamic parameters and system performance in different configurations using both models. They found that using the second model allows for the investigation of resonance phenomena. They also showed using the second model that the symmetrical arrangement of transducers has a higher performance than their asymmetrical model in a wave farm. Chang et al. [11] in 2015 conducted a theoretical study (two-dimensional potential theory) on wave energy absorption by an OWSC in order to examine it. They utilized the obtained results to validate their SPH simulations, demonstrating that the SPH method is a reliable approach for the design and optimization of an OWSC. Ferrer et al. [12] in 2016 conducted a numerical investigation on the slamming wave effect on the OWSC using the OpenFOAM software. They investigated the effects of fluid compressibility in the flow by employing both compressible and incompressible flow assumptions and compared the obtained results. The results indicated that the incompressible flow assumption provided sufficient accuracy, and there was no need to use the compressible flow assumption, given appropriate discretization. Wilkinson et al. [13] in 2017 conducted an experimental investigation on an an OWSC (1:30) with a modular flap under regular waves, comparing it with an OWSC with a rigid flap. In this model, they used the simplest form of damping, which is uniform damping for each module (each component of the flap). They demonstrated that the modular structure for the OWSC has advantages such as improved WEC performance, reduced forces on the foundation, and decreased construction and installation costs. The modular flap generates 23% more total power compared to the equivalent rigid flap. Jiang et al. [14] in 2018 investigated the hydrodynamic response of an OWSC along with various linear and nonlinear PTO systems. They also optimized the performance of the PTO systems aiming to enhance the performance of an OWSC, for this purpose, they employed a PTO simulation platform capable of generating different types of damping forces. The comparison of the WEC's efficiency under linear and nonlinear PTO damping has shown that the nonlinear PTO does not provide a significant advantage in power output. However, it exhibits better stability. Brito et al. [15] in 2019 examined the performance of an OWSC using numerical simulations in the SPH software, taking into account existing mechanical constraints, including the PTO system's compliance and flap inertia. The results indicated that the simulated numerical model accurately predicts the dynamics of the WEC. Brito et al [16] also in 2020 studied the 1:10 scale OWSC experimentally, taking into account the effects of the PTO system. Additionally, they proposed a mathematical model for PTO, The results indicated a weak correlation between the WEC's performance and its hydrodynamic response. Therefore, it does not necessarily imply that the maximum performance coincides with the peak hydrodynamic response. Liu et al. [17] in 2020 conducted a numerical investigation on cylindrical OWSC under the influence of regular waves

using the SPH method. They initially performed a comparison between the performance of cylindrical and rectangular flaps. It was determined that cylindrical flaps exhibit higher efficiency. Then, they proceeded to investigate the effects of five parameters on the WEC's performance, these parameters included the total mass of the flap, the distance between the Hinge and seabed, the damping of the PTO system, and the thickness of the flap. The numerical results indicated that the higher mass of the flap, thinner thickness, and more distance between the hinge and seabed contribute to improving the performance of the WEC. They also demonstrated that by increasing the damping of the PTO system, the WEC's performance initially increases and then decreases. Cheng et al. [18] in 2020 conducted a numerical study on an OWSC, including power extraction, efficiency, and hydrodynamic response. They found that as the wave amplitude increases, the hydrodynamic response amplitude operator (RAO) and performance decrease. Their results also showed that appropriate design of the hydrodynamic coefficients can create a resonance region, which can be beneficial in achieving maximum effective performance. Liu et al. [19] in 2022 studied the resonance phenomenon in an OWSC under regular waves using the boundary element method and investigated the correlation between the resonance phenomenon and the WEC's capture width ratio (CWR). The results showed that the maximum power absorption period is closer to the maximum angular velocity period than the natural period of the flap, and thus the maximum CWR does not occur during the resonance phenomenon. This paper provides an experimental analysis of the performance of an OWSC (1:8) specifically designed for the Caspian Sea. Given that most studies are conducted without accounting for scaling factors, this study investigates the performance and hydrodynamic behavior of the WEC at optimized draft depth by analyzing the pressure, damping, and transmission coefficients. Furthermore, the effect of wave characteristics and draft depth on the hydrodynamic coefficients were also investigated in terms of correlation.

2. System Description

2.1. Physical model

OWSC system has been designed and constructed. A schematic view of the system located in the wave flume of the Sea-Based Energy Research Group at Babol Noshirvani University of Technology has been shown in figure 1 [20] wave prob and system's dimensions have been presented by authors in [21, 22]. The PTO system and it's components are also showed in figure 2.

(a) (b)

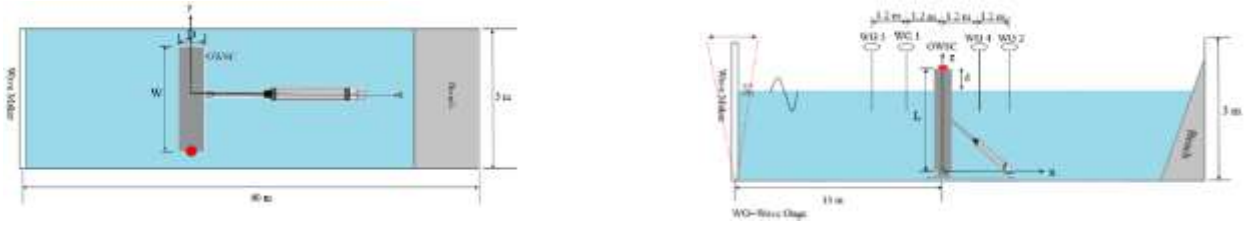

Figure 1. a model of an OWSC in a wave flume. a) top view b) side view

(a) (b)

Figure 2. a) a view showing the OWSC model b) schematic of OWSC and PTO system

To measure the angular displacement of the flap (θ), a tracker index has been used on the flap and a camera. It should be noted that the camera is installed in a suitable location with sufficient range to capture the large range of flap displacements. The location of the camera and other measuring equipment can be seen in Figure 3.

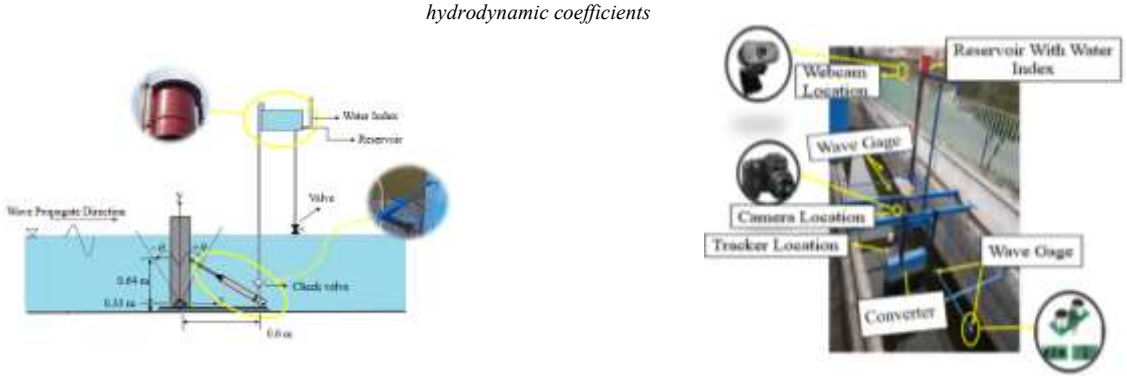

Figure 3. Location of camera and other measuring equipment

Figure 4. Views showing the OWSC model

In Figure 4, views of the OWSC model can be seen. For get more information about the system description, can refer to another work of the author [23].

3. Experimental Study

Froude scaling can be used to simulate the conditions of sea waves on a laboratory scale; according to the study conducted by Alamian et al. [24] on the conditions of waves in Caspian Sea, the selected wave conditions were a wave period range of [4-6] s and a wave height range of [0.5-1] meters, representing waves with the highest energy density.

Table 1. Laboratory conditions of waves

Frequency (Hz)	Wave height (m)	Depth (m)
0.4		0.8
0.43		0.9
0.47	0.04	1
0.50	0.06	1.1
0.53	0.08	1.2
0.57	0.1	1.3
0.60		1.4
0.63		1.5

Using Froude scaling, these conditions were converted to laboratory scale, the design parameters of the test were considered as Table 1.

4. Experimental Modeling

Based on the conducted studies, the parameters that affect the performance of an OWSC have been identified as the wave height (Hi), the pressure difference created in the PTO system (Δp), the flow rate in PTO system (Q), and the angular displacement (θ) (Eq.(1)):

$$P_{OWSC} = f(h, H_i, \theta, g, \rho, \Delta p, Q, d) \quad (1)$$

Where d represents the hydraulic cylinder diameter, ρ denotes the water density, and g refers to the gravitational acceleration. After the non-dimensionalization of the variables using the Pi-Buckingham theory, the following dimensionless hydrodynamic coefficients were extracted.

$$C_d = \frac{d^2 \sqrt{\frac{\Delta P}{\rho}}}{Q} \quad (2)$$

$$C_P = \frac{\Delta P}{\rho g H_i} \quad (3)$$

$$C_t = \frac{h\theta}{H_i} \quad (4)$$

Dimensionless damping coefficient of the OWSC (Cd), Where Cd is the dimensionless damping coefficient of the OWSC; the Cd shows the relationship between flow

rate and pressure in the PTO system. Dimensionless pressure coefficient has been shown by Cp and indicates the relationship between pressure inside the PTO system and incidence wave conditions, and the dimensionless transmission coefficient (Ct) shows the relationship between flap motion range and incidence wave conditions.

5. Governing Equations

In this section, the equations used to calculate each of the parameters are presented. In order to calculate the pressure difference created in the PTO system, Eq. (5) is used.

$$\Delta P = \frac{1}{2}\rho\left(V_1{}^2 - V_2{}^2\right) + \rho g h' \qquad (5)$$

Where V_1 is the water velocity at the reservoir inlet, V_2 is the water velocity in the reservoir, and h' is the distance between the reservoir and the fluem bed. The equations used to calculate Q (the flow rate pumped by the PTO system) are presented in another paper of this study [23]. To calculate θ, the Tracker software, which is a software for analyzing physical motion in video files, was used; since the displacement obtained by the Tracker software is in centimeter, Eq. (6) was used to find the displacement angle in radians from the rotation radius (r):

$$\theta(rad) = \frac{y(cm)}{r(cm)} \qquad (6)$$

6. Laboratory Equipment and Data Collection

The equipment used in this study includes the ultrasonic sensor US-100, a camera, and a webcam. The specifications of these equipment are listed in Table 2; more information about these equipment, as well as their calibration and uncertainty, can be found in reference [23].

Table 2. Specifications of measurement equipment used

Image	Accuracy	Measurement Equipment
	Zoom: ×34 Precision: 921000 pixels Focal range: 5.22 to 765 millim	Video camera Nikon coolpix L830
	Distance: 2 to 450 cm precision: 1 mm	US-100 sensor
	Film speed: 30 FPS	ROTEL-RW120 web camera

7. Results and Discussion

In this section, three important dimensionless hydrodynamic coefficients, including the damping, pressure, and transmission coefficients, are evaluated to investigate the performance of an OWSC. These coefficients are calculated at each draft depth and the effects of changing the draft depth and wave conditions including wave height and frequency, are examined. For this purpose, the dimensionless parameters of draft depth ($\frac{d}{h}$) and wave frequency ($f = \frac{H\omega^2}{g}$) were used. The results indicate [23] that the WEC has higher performance at wave frequency and dimensionless draft depth (water depth) of 0.4 Hz and 0.59 (0.9 m). Therefore, in this section, with the aim of investigate the effects of changing water depth and wave height on the hydrodynamic coefficients of the WEC, the wave frequency is considered constant at 0.4 Hz. Furthermore, to evaluate the effect of wave frequency and wave height on these coefficients, the water depth was fixed at 0.9 meters. Damping coefficient is a measure of flow rate in PTO system. Figure 5 shows the effect of dimensionless draft depth on the C_d at different wave heights; as shown in Figure 5, there is a parabolic nonlinear relationship between the dimensionless draft depth and the C_d. Also it can be observed that at the optimal dimensionless draft, The value of C_d is minimum. This point indicates that reducing the damping coefficient at the optimal draft depth leads to improved performance of the WEC. Alternatively, rising the height of the wave results in a decrease in the C_d. The important point is that in the characteristic range of Caspian Sea waves, meaning low wave height, the damping coefficient of the WEC is higher than in seas with high wave height.

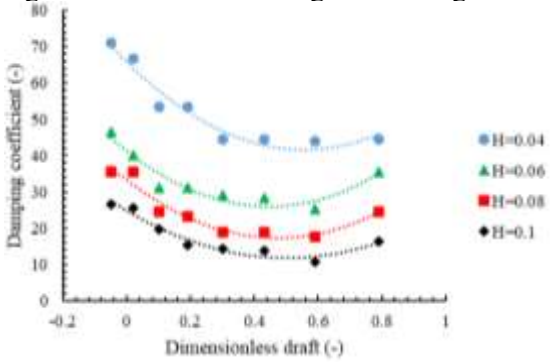

Figure 5. Dimensionless draft depth effect on damping coefficient

Figure 6 shows the variations of the pressure coefficient of the WEC with the change of dimensionless draft depth in different wave heights. As can be seen from the figure, the effect of the dimensionless draft depth on C_p is negligible, but the increase in wave height leads to a decrease in the C_p; the reason for this is that the pressure coefficient is inversely related to wave height and directly related to pressure changes within the WEC. Since the effect of the wave height is greater than the effect of pressure

changes within the WEC, an increase in the wave height leads to a change in the pressure coefficient.
The reason for this is that the C_p has an inverse relationship with the wave height and a direct relationship with the pressure change inside the WEC, since the effect of wave height is greater than the effect of pressure changes within the WEC, an increase in wave height results in a change in the C_p.

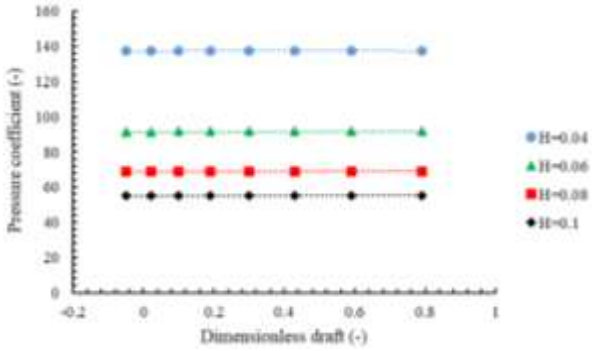

Figure 6. Dimensionless draft depth effect on pressure coefficient

One of the important dimensionless hydrodynamic coefficients in this study is the transmission coefficient of the WEC. Figure 7 shows the changes in the transmission coefficient with the change of dimensionless draft depth in different wave heights. As can be seen from Figure 7, an increase in the dimensionless draft depth leads to an increase in the transmission coefficient of the WEC. It is important to note that the C_t at the optimal dimensionless draft depth has larger values compared to other draft depth.

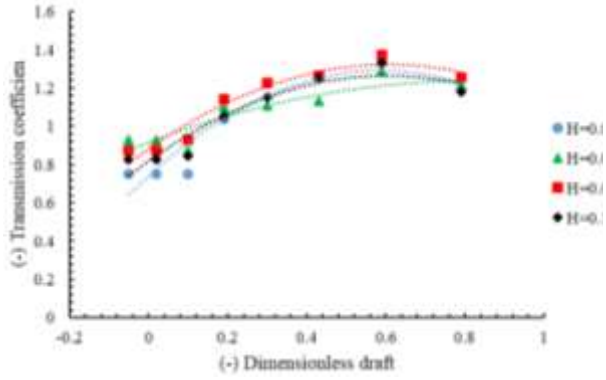

Figure 7. Dimensionless draft depth effect on transmission coefficient

In the following, the water depth is constant; the relationship between the dimensionless wave frequency and the C_d is shown in Figure 8. The results show that as the dimensionless wave frequency increases, C_d increases, one of the reasons for this is that with an increase in frequency, the WEC loses its ability to adapt to the wave and cannot complete a full Course of rotation.

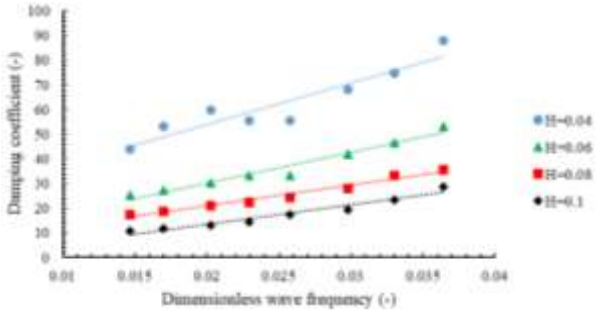

Figure 8. Dimensionless wave frequency effect on damping coefficient

Figure 9 examines the effect of dimensionless wave frequency on the C_p. It can be concluded that the dimensionless wave frequency has not much effect on the C_p, but the change in the wave height can be effective by considering the wave height in the denominator. As a result, the pressure coefficient decreases by approximately 40% when the wave height changes from 0.04 m to 0.1 m.

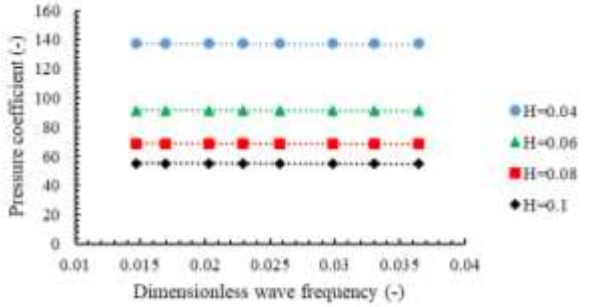

Figure 9. Dimensionless wave frequency effect on pressure coefficient

Figure 10 shows the effect of dimensionless wave frequency on the transmission coefficient. From Figure 10, it can be seen that the C_t decreases with increasing dimensionless wave frequency. This decrease is more severe at the lowest wave height than at other heights. On the other hand, if the wave height is between 0.06 m and 0.08 m, the transmission coefficient has higher values than at other wave heights.

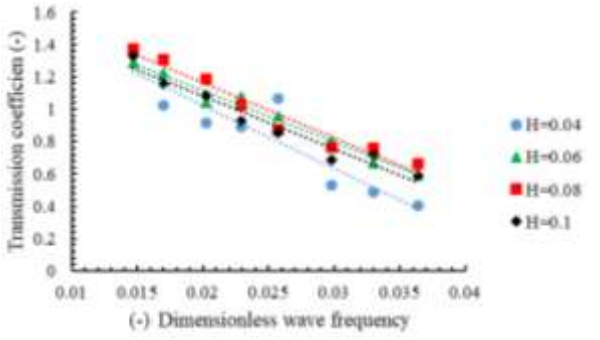

Figure 10. The effect of the dimensionless wave frequency on the transmission coefficient

Given the importance of the transmission coefficient of the WEC, its average values at different wave heights have been calculated and are presented in Figure 11. It

is found that changes in wave height can cause nonlinear behavior in the C_t. The C_t is small for both low and high wave heights, while it reaches its maximum value in the range of 0.07-0.08 m wave height. This point is essential from a structural considerations as it indicates that in the design of the structure, the flap displacement should be considered for this range of wave heights, rather than only for the maximum wave height.

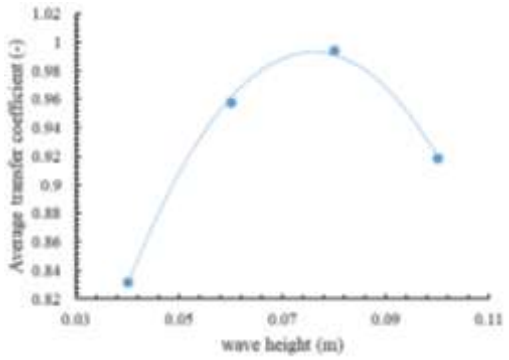

Figure 11. Variation of the transmission coefficient with wave height

To investigate the relationship between two parameters, their correlation can be examined. As shown, if the correlation is close to one, the two parameters are strongly directly related, meaning that an increase in one parameter or variable leads to an increase in the other variable. If the correlation is close to -1, the two parameters have an inverse relationship. This section presents the correlation between dimensionless draft depth, wave height, and the damping, pressure, and transmission coefficients, as shown in Table 3. Table 3(a) shows the negative correlation between the dimensionless draft depth and the C_d, indicating that an increase in draft depth results in a decrease in damping. Additionally, a stronger negative correlation is observed between wave height and C_d, which is 54% stronger. In Table 3 (b), the correlation between the dimensionless draft depth, wave height, and pressure coefficient is shown. The C_p has a very low correlation with the draft depth, almost equal to zero, meaning that the change in the dimensionless draft depth does not have much effect on the C_p. However, the correlation between wave height and the C_p is negative, near -1, indicating that the C_p decreases significantly as wave height increases.

Table 3. The correlation between the dimensionless submergence depth and collision wave height with coefficients a) transmission, b) pressure, c) damping

(a)

	d/h	Ct	H
d/h	1.000		
Ct	0.813	1.000	
H		0.070	1.000

(b)

	d/h	Cp	H
d/h	1.000		
Cp	0.001	1.000	
H		-0.965	1.000

(c)

	d/h	Cd	H
d/h	1.000		
Cd	-0.337	1.000	
H		-0.844	1.000

To better examine the correlation values for wave height and dimensionless draft depth separately, Figure 12 has been plotted; it is clear that the correlation between wave height and C_t is close to zero, and between wave height and C_d and C_p is close to -1. This indicates the importance of the wave height for the C_d and C_p and its low importance for the C_t. One of the important points in this figure is the high dependence of the transmission coefficient and damping coefficient (compared to the C_p) on the dimensionless draft depth and the lack of correlation between the C_p and the dimensionless draft depth.

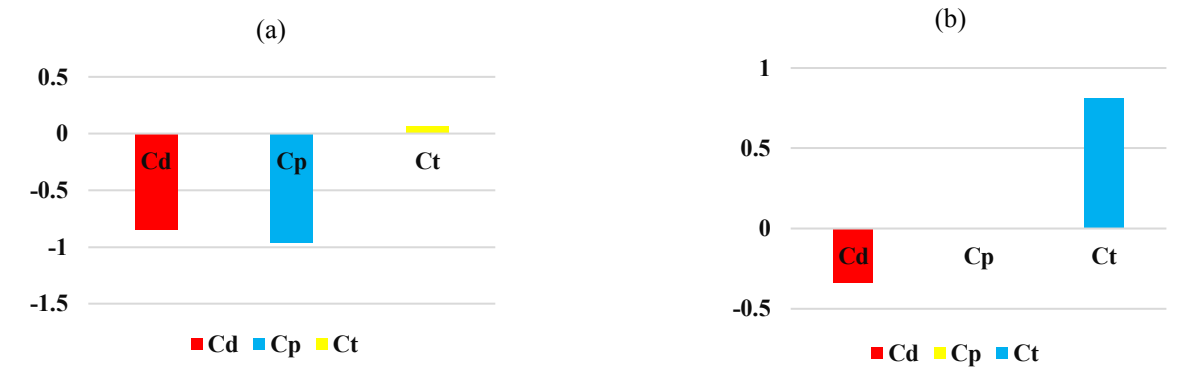

Figure 12. The correlation between a) wave height with damping, pressure, and transmission coefficients, b) dimensionless draft depth with damping, pressure, and transmission coefficients

8. Conclusions

In the evaluation of a WEC's performance, extracting dimensionless hydrodynamic coefficients is of great importance. Furthermore, investigating the effective parameters on these dimensionless coefficients can contribute to a better understanding of the WEC's performance and help identify conditions in which the WEC achieves its highest level of performance. In this paper, after defining the important dimensionless hydrodynamic coefficients of a model of the OWSC, including the damping, pressure, and transmission coefficients, they were calculated at different water depths. The effect of parameters such as dimensionless draft depth and wave conditions on these coefficients has been discussed. Finally, in order to examine the relationship of each coefficient with the draft depth and wave height, the correlation of dimensionless draft depth and wave height with each coefficient has been calculated and evaluated.

The results show that by analyzing these dimensionless coefficients, a better understanding of the performance of an OWSC can be achieved, and the analysis of the stated coefficients can be used in the design of this WEC, the analysis of these dimensionless coefficients can be utilized in summary, the main results of the study are as follows:

• As the wave height increases, the damping of the WEC decreases; the WEC exhibits higher damping coefficients for lower wave heights compared to higher wave heights.

• Water depth can affect the Cd has a nonlinear effect of the parabolic type and the minimum damping of the OWSC occurs at the optimized water depth, which shows that reducing the damping coefficient leads to better performance of the WEC.

• An increase in the wave height leads to a decrease in the dimensionless pressure coefficient; the reason for this is that the pressure coefficient has an inverse relationship with the wave height and a direct relationship with the pressure difference inside the WEC, and since the effect of the wave height is greater than the effect of the pressure changes in the OWSC, as a result, increasing wave height causes to a change in the pressure coefficient. The pressure coefficient decreases by approximately 40% when the wave height changes from 0.04 m to 0.1 m.

• The increase in dimensionless draft depth has resulted in an increase in the transmission coefficient; an important point to note is that the transfer coefficient at the optimum draft depth primarily has a larger value compared to other draft depths.

• Wave frequency can make damping coefficient rising; because it could be that with the increase in the wave frequency, the WEC loses the opportunity to adapt itself to the wave and consequently it cannot complete a full course, which increases the WEC's damping coefficient

• Wave frequency can decrease the transmission coefficient; but this decrease is more intense at the lowest wave height compared to other wave heights, on the other hand, if the wave height is between 0.06 to 0.08 m, the transmission coefficient has larger values compared to other wave heights.

• The wave height can lead to a non-linear behavior in the transmission coefficient, the transmission coefficient at small wave heights and large wave heights has a small amount while the transmission coefficient in the range of 0.07 to 0.08 m has reached its maximum value, from a structural considerations of view, this can be very important.

9. References

[1] A. J. Henry, "The hydrodynamics of small seabed mounted bottom hinged wave energy conerverters in shallow water," Queen's University Belfast, 2009.

[2] M. H. Jahangir, M. Mazinani, and Z. Ranji, "The Application of Energy Absorbers to Harness Wave Energy in the Caspian Sea: A Feasibility Study," *International Journal Of Coastal, Offshore And Environmental Engineering (ijcoe),* vol. 6, no. 5, pp. 39-50, 2021.

[3] M. Aghanezhad, R. Shafaghat, and R. Alamian, "Experimental Performance Evaluation of a Hydraulic PTO System for Centipede Wave Energy Converter," *International Journal Of Coastal, Offshore And Environmental Engineering (ijcoe),* vol. 5, no. 4, pp. 35-46, 2020.

[4] M. Folley, T. Whittaker, and M. Osterried, "The oscillating wave surge converter," in *ISOPE International Ocean and Polar Engineering Conference*, 2004: ISOPE, pp. ISOPE-I-04-073.

[5] B. Drew, A. R. Plummer, and M. N. Sahinkaya, "A review of wave energy converter technology," ed: Sage Publications Sage UK: London, England, 2009.

[6] A. Babarit, J. Hals, M. J. Muliawan, A. Kurniawan, T. Moan, and J. Krokstad, "Numerical benchmarking study of a selection of wave energy converters," *Renewable energy,* vol. 41, pp. 44-63, 2012.

[7] E. Renzi and F. Dias, "Hydrodynamics of the oscillating wave surge converter in the open ocean," *European Journal of Mechanics-B/Fluids,* vol. 41, pp. 1-10, 2013.

[8] D. Sarkar, E. Renzi, and F. Dias, "Wave power extraction by an oscillating wave surge converter in random seas," in *International*

Conference on Offshore Mechanics and Arctic Engineering, 2013, vol. 55423: American Society of Mechanical Engineers, p. V008T09A008.

[9] Y. Wei, A. Rafiee, B. Elsaesser, and F. Dias, "Numerical simulation of an oscillating wave surge converter," in *International Conference on Offshore Mechanics and Arctic Engineering*, 2013, vol. 55317: American Society of Mechanical Engineers, p. V001T01A012.

[10] E. Renzi, A. Abdolali, G. Bellotti, and F. Dias, "Wave-power absorption from a finite array of oscillating wave surge converters," *Renewable Energy,* vol. 63, pp. 55-68, 2014.

[11] Y.-C. Chang, D.-W. Chen, Y.-C. Chow, S.-Y. Tzang, C.-C. Lin, and J.-H. Chen, "Theoretical analysis and sph simulation for the wave energy captured by a bottom-hinged owsc," *Journal of Marine Science and Technology,* vol. 23, no. 6, p. 9, 2015.

[12] P. Ferrer, D. Causon, L. Qian, C. Mingham, and Z. Ma, "Numerical simulation of wave slamming on a flap type oscillating wave energy device," *Proceedings of the Twentysixth,* 2016.

[13] L. Wilkinson, T. Whittaker, P. R. Thies, S. Day, and D. Ingram, "The power-capture of a nearshore, modular, flap-type wave energy converter in regular waves," *Ocean Engineering,* vol. 137, pp. 394-403, 2017.

[14] X. Jiang, S. Day, and D. Clelland, "Hydrodynamic responses and power efficiency analyses of an oscillating wave surge converter under different simulated PTO strategies," *Ocean Engineering,* vol. 170, pp. 286-297, 2018.

[15] M. Brito *et al.*, "A numerical tool for modelling oscillating wave surge converter with nonlinear mechanical constraints," *Renewable Energy,* vol. 146, pp. 2024-2043, 2020.

[16] M. Brito, R. M. Ferreira, L. Teixeira, M. G. Neves, and R. B. Canelas, "Experimental investigation on the power capture of an oscillating wave surge converter in unidirectional waves," *Renewable Energy,* vol. 151, pp. 975-992, 2020.

[17] Z. Liu, Y. Wang, and X. Hua, "Numerical studies and proposal of design equations on cylindrical oscillating wave surge converters under regular waves using SPH," *Energy Conversion and Management,* vol. 203, p. 112242, 2020.

[18] Z. Liu, Y. Wang, and X. Hua, "Prediction and optimization of oscillating wave surge converter using machine learning techniques," *Energy Conversion and Management,* vol. 210, p. 112677, 2020.

[19] Y. Cheng, G. Li, C. Ji, T. Fan, and G. Zhai, "Fully nonlinear investigations on performance of an OWSC (oscillating wave surge converter) in 3D (three-dimensional) open water," *Energy,* vol. 210, p. 118526, 2020.

[20] Y. Liu, Y.-H. Cho, N. Mizutani, and T. Nakamura, "Study on the resonant behaviors of a bottom-hinged oscillating wave surge converter," *Journal of Marine Science and Engineering,* vol. 10, no. 1, p. 2, 2022.

[21] G. Sadripour, R. Shafaghat, B. Alizadeh Kharkeshi, and S. Sadeqi, "Experimental Study on The Effect of Water Depth and Incident Wave Frequency on The Performance of a OWSC Imposed to Caspian Sea Wave Conditions," *Modares Mechanical Engineering,* vol. 22, no. 9, pp. 603-613, 2022.

[22] G. Sadripour, R. Shafaghat, B. Alizadeh Kharkeshi, R. Tabassom, and A. Mahmoudi, "Installation Depth and Incident Wave Height Effect on Hydrodynamic Performance of a Flap Type Wave Energy Converter: Experimental Analysis," *International Journal of Engineering,* vol. 35, no. 12, pp. 2283-2290, 2022.

[23] R. Alamian, R. Shafaghat, S. S. Hosseini, and A. Zainali, "Wave energy potential along the southern coast of the Caspian Sea," *International journal of marine energy,* vol. 19, pp. 221-234, 2017.